TRUNCATED DUAL-CAP NUCLEATION SITE DEVELOPMENT

Douglas M. Matson and Paul J. Sander

Tufts University;
Department of Mechanical Engineering;
200 College Avenue; Medford, MA 02155, USA

Abstract

During heterogeneous nucleation within a metastable mushy-zone, several geometries for nucleation site development must be considered. Traditional spherical dual cap and crevice models are compared to a truncated dual cap to determine the activation energy and critical cluster growth kinetics in ternary Fe-Cr-Ni steel alloys. Results of activation energy results indicate that nucleation is more probable at grain boundaries within the solid than at the solid-liquid interface.

Introduction

Undercooled hypoeutectic ternary Fe-Cr-Ni steel alloys solidify in a two-step process known as double recalescence [1]. The metastable ferritic bcc-phase forms first with subsequent transformation to the stable austenitic fcc-phase. The delay between these two nucleation events represents the incubation time for the stable phase and this delay is a strong function of melt convection. In classical nucleation theory [12-14], the steady-state nucleation rate, I_S, and time dependent nucleation rate, I, are related by the equations

$$I = I_S \, \exp\left[-\frac{\tau}{t} \right] \qquad for \ \ I_S = I_O \, \exp\left[-\frac{\Delta G *}{k_B \, T} \right] \qquad (1)$$

where τ is a characteristic incubation time, t the observed delay time, I_O a pre-exponential factor, $\Delta G*$ the Gibbs free energy for formation of a critical nucleus of n* atoms of a pure material, and T the transformation temperature. The Boltzmann constant has a value of $k_B = 1.38 \times 10^{-23}$ J/atomK. Steady-state nucleation does not become appreciable until $\Delta G* > 60 \ k_B T$ while transient nucleation does not become appreciable until $t \gg \tau$. Turnbull estimated that for condensed phases the incubation time was a function of the size of the cluster and the rate at which atoms cross the interface, $\beta*$, between the surrounding matrix and the cluster [2].

$$\tau = \frac{(n*)^2}{\beta *} \qquad (2)$$

The attachment rate β* has variously been related to the jump frequency [2] and the lattice diffusivity [3-5]. By invoking the principle of time reversal, where the statistical fluctuations in cluster size follow the same path during growth and decomposition, Feder *et al* [6] determined the incubation time to be

$$\tau = \frac{-4\,k_B\,T}{\beta * \left.\dfrac{\partial^2(\Delta G)}{\partial n^2}\right|_{n*}}$$

(3)

Russell [7] evaluated condensed phase nucleation for binary systems to account for the influence of solute partitioning and found that clusters approaching the critical size were surrounded by an enriched solute shell, contrary to expectation, and that diffusivity of the slower moving species controls the attachment rate with an interchange frequency β'.

$$\beta' = \frac{x}{a_o^2}\left(\frac{2\,D_A\,D_B}{D_A + D_B}\right) \qquad \text{for } x = C_A\left(\frac{A_S}{a_o^2}\right)$$

(4)

where x is the number of atoms jumping a jump distance a_o and the subscripts on the diffusivity D represent solute A and solvent B. The number of atoms jumping can be evaluated from the surface concentration C_A, the interface area A_S, and the area per atom. A key finding for multi-component systems is that the rate controlling step for linked flux evaluations is replacement of shell atoms of the controlling species and not the interfacial jump frequency.

In an effort to identify the mechanism for stable-phase nucleation in ternary Fe-Cr-Ni steel alloys, Koseki [1] showed that a dual cap cluster forming within the metastable solid along a bcc-bcc boundary was more probable than (1) homogeneous nucleation of a sphere in the melt, (2) heterogeneous nucleation as a single spherical cap protruding from the bcc-solid and into the melt, (3) heterogeneous nucleation of a spherical cap protruding into the solid, and (4) heterogeneous nucleation of a dual cap along the solid-liquid interface. In these analyses, the time to form a potential nucleation site is taken as zero. Homogeneous nucleation in the melt requires no site development time. Homogeneous nucleation within the solid and heterogeneous nucleation in the form of a spherical cap at the solid-liquid interface requires only that the pre-existing solid exist. Since the solid/liquid interface forms immediately during primary recalescence there is no delay for site formation.

A transient site, such as the solid-solid grain boundary dual cap, is one that forms sometime after primary solidification. Two processes become important in the evaluation of transient site development. First, we must assess how long it takes to form a suitable heterogeneous nucleation site and then, second, we must define how long it takes for a critical nucleus to grow after a suitable site has formed. The sum of these two events determines the incubation period which corresponds to the delay time between primary metastable recalescence and subsequent initiation of the conversion to the stable phase.

Hanlon [8] proposed that fluid drag and dendrite bending can lead to secondary arm collision which will create the required bcc-bcc grain boundary. Matson [9] extended these analysis by showing that nucleation of the stable phase could only occur once a suitable site had formed on,

or in, the pre-existing metastable solid thus explaining how convection can influence predictions using classical nucleation theory. Sites that form due to collision include the bcc-bcc grain boundary and the liquid-filled crevice formed by the intersection of two parallel cylindrical arms. Since the predicted delay time required for cluster growth for both the dual cap and crevice clusters was several orders of magnitude faster than the observed delay, the formation of the grain boundary crevice, and not cluster growth, was identified as the controlling process.

One additional geometry needs to be considered. The current paper looks at the potential for interaction between a dual cap and the liquid due to growth near the grain boundary/liquid interface. Dual cap cluster formation was primarily limited due to diffusion along the grain boundary since diffusion through the solid was sluggish and thus grain boundary diffusion dominated. The activation energy was low due to the favorable low surface/volume ratio. Crevice cluster formation was significantly more rapid due to enhanced diffusion through the surrounding liquid but the activation energy was higher due to an increase in surface/volume. The intersection of a dual cap with the liquid surface combines these processes and must be evaluated to complete the picture. The geometry that forms is known as a truncated dual cap.

Geometry of a truncated dual cap

A dual cap consists of two identical spherical sections with a characteristic intersection angle, 2θ, defined by the relative interfacial free energies, γ. Along the grain boundary mirror plane, equilibrium is maintained if

$$\gamma_{MM} = 2 \gamma_{MS} \cos \theta \tag{5}$$

with subscripts MM for metastable/metastable and MS for metastable/stable. The activation barrier at the critical radius, ΔG^*, is evaluated based on equating surface and volume terms, A and V respectively, at the critical cluster radius r* where $^{dG}/_{dn}$ goes to zero such that

$$\Delta G^*\big|_{r*} = 2 A_{MS} \gamma_{MS} - A_{MM} \gamma_{MM} - V \Delta G_V \tag{6}$$

$$\Delta G_V = \frac{\Delta H \ \Delta T}{T_m}$$

with ΔH the enthalpy of fusion, ΔT the undercooling set by the melting points of the metastable and stable phases, and T_m the melting point of the stable phase. The area and volume terms are readily evaluated from equations for spherical sections. If we assume typical values for thermophysical properties for steel alloys[9] to be $\gamma_{MM} = 0.468$ J/m^2, $\gamma_{ML} = 0.212$ J/m^2, $\gamma_{SL} = 0.302$ J/m^2, $\Delta G_V = 2.56 \times 10^7$ J/mol, $D_{GB} = 1 \times 10^{-10}$ m/s^2, $D_S = 1 \times 10^{-14}$ m/s^2, $D_L = 3 \times 10^{-9}$ m/s^2, and a grain boundary thickness of t = 5 Å, then the angle is $2\theta = 41.2°$, the activation barrier is $^{\Delta G^*}/_{kT} = 102$ for a nucleus containing 15000 atoms with a delay time of $\tau = 5.9 \times 10^{-8}$ sec.

Note that the value for the interfacial free energy between stable and metastable phases is highly speculative given the inability to experimentally define this value. Thus a value of $\gamma_{MS} = 0.250$ J/m^2 was selected as representative. Throughout the remainder of this paper, the errors associated with this selection are investigated.

When a dual cap intersects the liquid, the common circular basal surface is truncated. This is shown in Figure 1 where the overall shape of the transformed volume is seen in (a) and each of the three sub-volumes which comprise the shape are visually blown apart in (b). Note that top and bottom represent the converted section of the dual cap within the metastable solid while the pointed ellipsoid extends out into the liquid.
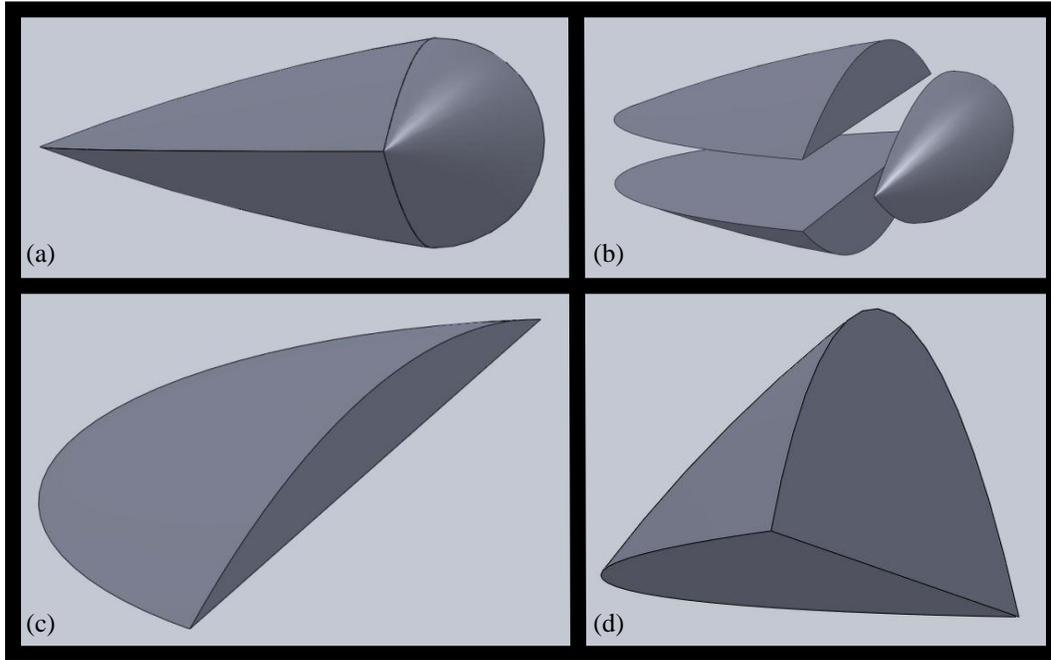
Figure 1. Geometry of a truncated dual cap. (a) overall volume (b) exploded view to show upper and lower truncated cap sections and the ellipsoid protruding out into the liquid (c) truncated cap for typical properties and $\gamma_{MS} = 0.25$ J/m^2 (d) truncated cap for typical properties and $\gamma_{MS} = 0.37$ J/m^2

In Figure 1 the influence of the value of the interfacial free energy between metastable and stable phases is illustrated where in (c) the interfacial free energy is set at $\gamma_{MS} = 0.25$ J/m^2 while in (d) $\gamma_{MS} = 0.37$ J/m^2. Of particular interest is the strong influence of the value of the γ_{MS} parameter on the ellipsoid dimensions. As seen in Figure 1(c), at low values the interfacial properties dominate and the point where metastable solid/metastable solid/liquid are in equilibrium is pronounced. In Figure 1(d) the volume properties dominate and the point is less pronounced. This point is of critical concern because at this location surface frustration, a local instability caused by anisotropy of surface tension, causes modeling of the geometry to break down. Isotropic interfacial energies require that the boundary between metastable solid and liquid have the same wetting angle which means that the "ellipsoid" should, in fact, be a spherical cap section with a-axis and b-axis the same. This is certainly not true in (c) but the

geometry comes closer to this shape in (d). Surface frustration is due not only to the elliptical cross-section of this face but also due to the definition of surface angles.

Along the solid/solid interface (left side of the shape) equation 5 is used to define the interior angle 2θ relative to the horizontal mirror plane as before. At the point where the metastable solid-solid boundary intersects the liquid-stable solid boundary (the point in the ellipsoid) the interfacial free energy balance results in the definition of two equations in two unknowns along horizontal and vertical axes

$$\gamma_{LM} = \gamma_{MS} \cos \theta_S + \gamma_{LS} \cos \theta_L \tag{7}$$

$$\gamma_{MS} \sin \theta_S = \gamma_{LS} \sin \theta_L \tag{8}$$

These define the angle the truncated section makes to the vertical, θ_S, and the angle the exterior surface of the ellipsoid makes to the vertical, θ_L. Note that ideally the angle should be identical along the a-axis and b-axis of the ellipsoid but surface frustration makes this not possible due to the required existence of the pointed intersection. To estimate the surface area and volume it was assumed that the shape could be represented by rotating the destroyed metastable solid-liquid interface about the solid-solid line resulting in a shape similar to half a football.

The truncated dual cap and ellipsoid shapes cannot be characterized readily analytically and a graphical approach was used to estimate areas and volumes. Using the predicted characteristic lengths and angles, a model was developed in SolidWorks® to evaluate areas and volumes as a function of the interfacial free energy γ_{MS}. Defining the base of the truncated cap as A_{MM}, the front as A_{ML}, the surface as A_{MS}, and the exterior of the ellipsoid as A_{SL}, the activation barrier can be evaluated from

$$\Delta G *\big|_{r*} = 2 A_{MS} \gamma_{MS} + A_{SL} \gamma_{SL} - 2 A_{ML} \gamma_{ML} - A_{MM} \gamma_{MM} - V \Delta G_v \tag{9}$$

Using typical thermophysical properties presented earlier, $\theta = 41.2°$, $\theta_S = 81.2°$, $\theta_L = 54.9°$, and the ellipsoid has major axis length a = 19.9 x10^{-9} m and minor axis length b = 3.3 x10^{-9} m. The activation barrier is calculated to be $\Delta G*/kT = 3315$ for a nucleus containing 156000 atoms with a delay time of $\tau = 2.8$ x10^{-9} sec. The results of calculations of this type for all three mechanisms as defined over the entire range of possible interfacial free energies are presented in Figure 2 and Figure 3.

Discussion

Prediction results show that all three mechanisms are possible but only for low values of the interfacial free energy. At these energies, the shape of both the dual cap and truncated dual cap are thin saucer-shaped volumes due to the small interior angle along the metastable solid grain boundary. The truncated portion thus has a highly anisotropic elliptical shape with major axis to minor axis ratio varying from 11 to around 6 over the range of interfacial free energies investigated. The sensitivity to selection of values for interfacial energies can readily be investigated beyond what has been presented here as part of a larger evaluation of error associated with use of this type of technique. For example, if the value of the interfacial free energy of the metastable solid-solid boundary is reduced from the nominal value of $\gamma_{MM} = 0.468$

J/m^2 to γ_{MM} = 0.212 J/m^2 (the value for γ_{ML}) then major to minor axis ratio is reduced to around 1.6 and is insensitive to the selection of γ_{MS}. This ratio represents geometries closer to the desired isotropic, circular shape. Note that all interfacial free energy values have a high inherent uncertainty and thus the results should be viewed as indicating trends and not as numerical predictions. Results are ordinal and not cardinal.
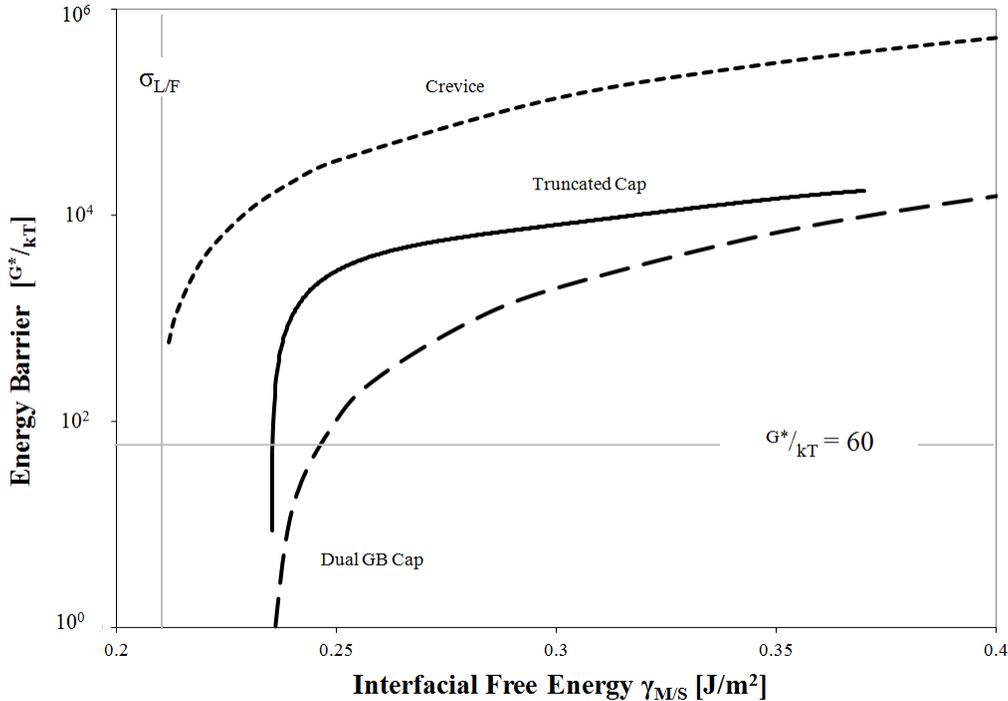
Figure 2. Energy barrier for nucleation of each cluster shape over the range of possible interfacial free energy values.

Figure 2 also clearly shows that the truncated cap geometry does successfully combine elements of both the solid-solid dual cap mechanism and the solid-liquid crevice mechanism. Predictions for the truncated dual cap tend to lie between the extremes calculated for the other two mechanisms however if all were operational this mechanism would dominate since the *fastest possible* mechanism is favored and the truncated cap is kinetically fastest over the entire range, as seen in Figure 3. However, since the energy barrier is higher for the truncated dual cap than for the embedded dual cap it is unlikely to be operative except at interfacial free energies less than a value of around γ_{MS} = 0.24 J/m^2.

One additional weakness of the approach used to estimate the surface area and volume for the pointed ellipsoid section for this geometry is that in order to obtain a tractable solution for the ellipsoid form, the foot-ball shaped rotation element was selected. This technique was used because SolidWorks® can readily generate this shape. Unfortunately, this ignores the calculated angle θ_L= 54.9° for γ_{MS} = 0.25 J/m^2 which should be constant along the three-phase interface.
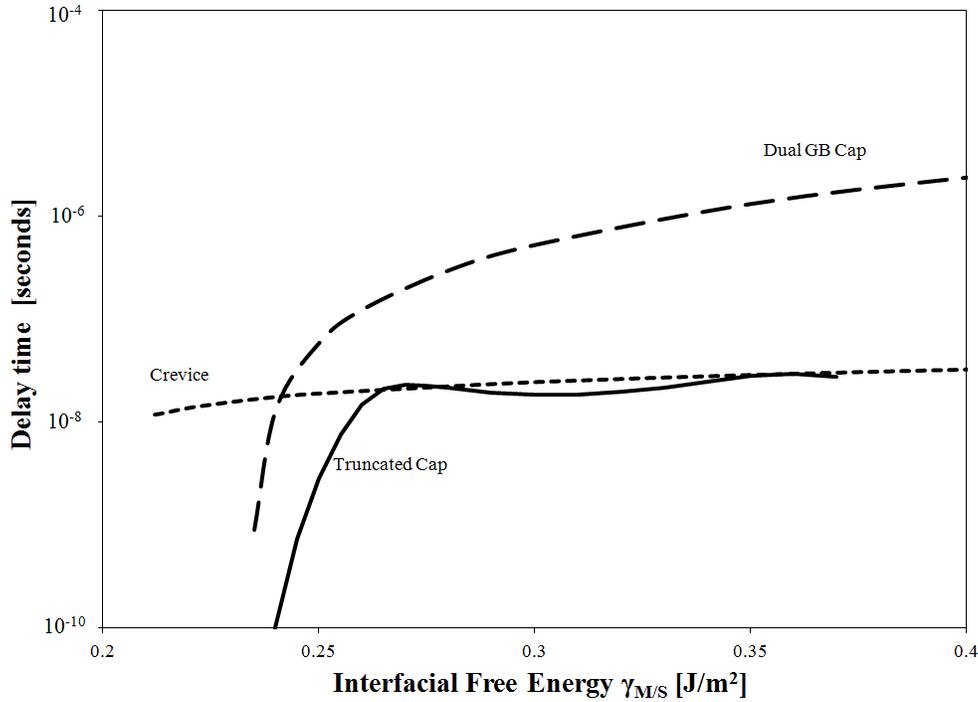
Figure 3. Kinetics of cluster formation for each shape over the range of possible interfacial free energy values.

Note that the rotated shape has a continuously changing surface angle. The extremes occur at the point along the major axis where the angle is $\theta_L^{min}= 18.9°$, and at the top along the minor axis where the angle is $\theta_L^{max}= 90°$. The effect of this change in angle is a continuously changing curvature of the surface which, as previously noted, results in surface frustration. This warping of the ideal geometry also results in a slight overestimation of the surface area and volume – estimated to be on the order of 37% and 58% respectively for these conditions – with the error decreasing because the difference between major and minor axis decreases significantly with increasing γ_{MS}. One interesting result of this surface frustration is that the decreased angle at the point strains the equilibrium at the three-phase junction and creates an additional resistance to cluster formation. This effect is commonly observed by children blowing up a balloon – if a strain is induced along one axis by pinching, the increase in anisotropic surface tension only allows expansion of the balloon along orthogonal axes. Thus for our application there is a strain term which must be added to the free energy balance and growth along the major axis is hindered. The polarity of this term suggests that the resulting activation energy will be greater than anticipated. These observations further strengthen the conclusion that clusters will form along the grain boundary within the metastable solid and not at the intersection of the metastable boundary and the undercooled liquid.

These theories must be validated over a wide range of convection conditions as is only possible through electromagnetic levitation experimentation in microgravity [10].

Summary

Evaluation of the predicted delay times for all mechanisms shows that the incubation time to grow a critical cluster is several magnitudes faster than observed. This supports the theory that, following formation of the metastable array, the controlling kinetic mechanism is formation of a site where nucleation may occur rather than growth of a critical cluster. Evaluation of the energy barrier indicates that over a select and limited range of interfacial free energy values, all of the mechanisms – spherical cap, crevice nucleation, and truncated cap – are possible. However, since the barrier for formation of a truncated cap is greater than that for a dual cap for all interfacial energies evaluated in this study, cluster formation is more likely along a grain boundary within the solid rather than at the intersection of the boundary and the liquid.

References

1. T. Koseki and M. C. Flemings, "Solidification of undercooled Fe-Cr-Ni alloys: Part I. Thermal behavior" *Metall. Mater. Trans.* A26[11] (1995) 2991-2999.
2. J. H. Hollomon, D. Turnbull, "Nucleation", *Prog. Met. Phys.* **4**, (1953) 333-338.
3. D. Turnbull, J.C. Fisher, "Rate of nucleation in condensed systems", *J. Chem. Phys.* **17** (1949) 71-73.
4. R. Becker, "Nuclear formation in the separation of metallic mixed crystals" *Anal. Phys.* **32**[1-2] (1938) 128-140.
5. A. Kantrowitz, "Nucleation in very rapid vapor expansions", *J. Chem. Phys.* **19**, (1951) 1097-1100.
6. J. Feder, K. C. Russell, J. Lothe, G. M. Pound, "Homogeneous nucleation of droplets in vapours" *Adv. Phys.* **15** (1966) 111-178.
7. K. C. Russell, "Linked flux analysis of nucleation in condensed phases" *Acta Metall.* **16**, (1968) 761-769.
8. A.B. Hanlon, D.M. Matson, and R.W. Hyers, "Internal Convective Effects on the Lifetime of the Metastable Phase Undercooled Fe-Cr-Ni Alloys," *Philosophical Magazine Letters*, vol. 86, no. 3, (2005), 165-174.
9. D.M. Matson, "Ch 10 – Nucleation within the Mushy-zone", in *Solidification of containerless Undercooled Melts*, D. M. Herlach and D. M. Matson eds., Wiley-VCH, (2012) *in press*.
10. D.M. Matson, R. W. Hyers, T. Volkmann, and H.-J. Fecht, "Phase selection in the mushy zone: LODESTARS and ELFSTONE Programs", *Physics IOP*, Proceedings of *ISPS 2011 Conference*, July 14, 2011, Bad-Godesberg DE, (2011) *in press*.